Hindawi
Mathematical Problems in Engineering
Volume 2019, Article ID 7205154, 9 pages
https://doi.org/10.1155/2019/7205154

Research Article

Multi-Target Strike Path Planning Based on Improved Decomposition Evolutionary Algorithm

Ming Zhong, RenNong Yang, Jun Wu, and Huan Zhang

Air Force Engineering University, Xian 710038, China

Correspondence should be addressed to Ming Zhong; 707469602@qq.com

Received 5 September 2018; Revised 25 November 2018; Accepted 12 December 2018; Published 3 January 2019

Guest Editor: Love Ekenberg

Copyright © 2019 Ming Zhong et al. This is an open access article distributed under the Creative Commons Attribution License, which permits unrestricted use, distribution, and reproduction in any medium, provided the original work is properly cited.

This study proposes a path-finding model for multi-target strike planning. The model evaluates three elements, i.e., the target value, the aircraft's threat tolerance, and the battlefield threat, and optimizes the striking path by constraining the balance between mission execution and the combat survival. In order to improve the speed of the Multi-Objective Evolutionary Algorithm Based on Decomposition (MOEA/D), we use the conjugate gradient method for optimization. A Gaussian perturbation is added to the search points to make their distribution closer to the population distribution. The simulation shows that the proposed method effectively chooses its target according to the target value and the aircraft's acceptable threat value, completes the strike on high value targets, evades threats, and verifies the feasibility and effectiveness of the multi-objective optimization model.

1. Introduction

The air defense system has been significantly improved in modern warfare [1]. Air strikes from low altitude play an important role in modern warfare. The use of ground clutter cover and the existence of radar low altitude blind spots can greatly reduce the enemy's air defense capability and improve the penetration probability; however, the high risk and high operational difficulty of low altitude penetration limit the usability of low altitude penetration [2]. Path planning becomes one of the key technologies for precision strike.

Traditional models for path planning mainly evaluate the threat level due to terrain and air defense radar. These models minimize the threat through multi-objective algorithm [3], but seldom consider the situation of multi-target striking. In an actual combat, simply flying from a point A to a point B is not enough. Aircrafts often need to pass through multiple targets or areas extremely important for mission completion, such as the mission assembly area, the refueling area, and the targets to destroy. The ratio between the target value and its associated air defense capability varies for different targets. Therefore, it is necessary to plan the flying path that maximizes the probability of the target elimination as well as the aircraft's chance of survival.

In recent years, [4–6] proposed several modeling approaches that can plan flying paths connecting multiple target regions. The basic theory is to model the path planning problem as a traveling salesman problem (TSP) after the targets are chosen. Although these approaches can make the flying track pass through multiple target areas, there are two problems. Firstly, they do not rank the target according to its value. Secondly, path evaluation and aircraft safety are not considered. The path planned by these models will inevitably pass through the chosen target areas, even if the threat cost to these areas has exceeded the upper limit of the aircraft or a target is simply inaccessible. To solve the aforementioned problems, this paper proposes a path planning modeling approach for multi-target strike missions. It evaluates the balance among the aircraft might, the target value, and the threat level. It links the targets selection and the path evaluation. The evaluation is used to complete path planning under more complex mission conditions.

In our approach, the evolutionary algorithm is used to solve path planning [7, 8], and the decomposition multi-objective evolutionary algorithm (MOEA/D) [9] is used to solve the model. The simulation results show that the model is capable of completing the path planning effectively after weighing the target value and the threat.

2. Methodology

Given known conditions of the battlefield terrain, the air defense threat and the target location, an aircraft faces two kinds of threats: the terrain obstacle and the struck by the air defense system en route to target. Most of the targets in a battlefield are under the protection of an air defense system. The bombing aircraft is inevitably subject to a high level of air defense threats. The aircraft's risk tolerance is higher for higher value targets, and vice versa.

2.1. Function of Path. Within the mission domain, an aircraft flies from point A to point B before leaving the battlefield. Connecting point A and point B, the path of aircraft can be represented by Fourier series with AB as the axis,

$$y_i = \sum_{i=1}^{n} k_i \sin(\omega_i x_i), \tag{1}$$

where w_i, $(n = 1, 2, 3, ..., n)$ are the angular frequencies and k_i, $(n = 1, 2, 3, ..., n)$ are the corresponding amplitudes. The low frequency part of sine function is taken for the maneuverability. The minimum turning radius of an aircraft is $r_{\min}$.

$$r_{\min} = \frac{v^2}{g} \cdot \tan\theta_{\max}, \tag{2}$$

where v is the speed of the aircraft, g is the acceleration of gravity, and $\theta_{\max}$ is the maximum roll angle of the aircraft. Setting $v = 720km/h$ and $\theta_{\max} = 75^\circ$ gives a minimum turning radius $r_{min} = 1.1$km. The curvature radius of the path should be larger than the minimum turning radius r_{min}:

$$r_{\min} \le \left| \frac{\left(1 + k_{\max}^2 \times \cos^2(w)^{3/2}\right)}{k_{\max} \times \sin(w)} \right|. \tag{3}$$

The maximum amplitude is $k_{\max}$. Set $k_{\max} = 6$; the range of path angular frequency can be obtained according to Figure 1.

According to Figure 1, the range of available w is about

$$(0.04 + k\pi, 1.30 + k\pi) \cup (1.85 + k\pi, 3.10 + k\pi). \tag{4}$$

The amplitude range is 0<k<6. Within these frequency and amplitude ranges, we use the method in [1] to randomly generate a matrix of n×m. If m is the population size and n is the length of individual chromosome, k_i in each row of the amplitude matrix constitutes a chromosome. The gene location of chromosomes corresponds to the angular frequency, and the gene value is the corresponding amplitude. We next bring the angular frequency w and amplitude k into the path function and compute a fight path.

2.2. Constraint Analysis for Path Planning. The constraints on the path planning consist of four factors formulated as follows.

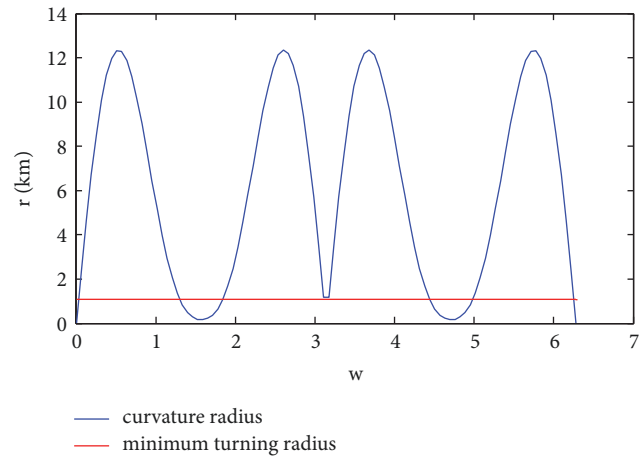

Figure 1: Curvature radius and minimum turning radius function.

(1) The path's length and offset: the path offset p is the distance between the path point (x_i, y_i) and the straight line from A to B.

$$p = \sum_{i=1}^{n} \frac{|x_i - y_i|}{\sqrt{2}}. \tag{5}$$

The path length S is

$$S = \int_{x_1}^{x_i} \sqrt{1 + y^2}\, dx. \tag{6}$$

(2) Terrain obstacles: if a single terrain obstacle can be transformed into a set of circles with different radii, the distance between the path point (x_i, y_i) and each circle $o_i(x_{oi}, y_{oi})$ should be greater than the radius r_{oi}.

$$\sqrt{(x_i - x_{oi})^2 + (y_i - y_{oi})^2} \ge r_i \tag{7}$$

(3) The threats from the air defense system: the air defense threats can be divided into two levels: the general threat area where the aircraft can be detected and shot down, and the serious threat area where the risk of being shot down dramatically increases. We set the threat values for each zone based on the zone's level of threat.

(4) The constraint on the targets: we set the coordinates of the targets to (x_{hi}, y_{hi}). In the case of dropping aerial bombs, an aircraft needs to face the target to ensure a successful bombing. The P is the horizontal distance between the aircraft location and the target point.

$$p = \sqrt{\frac{2h}{g}} \cdot v \tag{8}$$

where h is the altitude and v is the aircraft velocity. Since the aircraft is not guaranteed to face the target after entering the bombing zone, it needs to make some maneuvers to adjust its heading. Considering the various headings when entering the bombing zone, the aircraft should adjust its heading at the latest $R_{\min}$ from the target point,

$$R_{\min} = \sqrt{r_{\min}^2 + p^2}. \tag{9}$$

Therefore, in the initial stage of bombing, the aircraft should be in a ring with an outer diameter of $R_{\max}$ and an inner diameter of $R_{\min}$; $R_{\max} = R_{\min} + 1$. Let (x_h, y_h) be the target point; the path point (x_i, y_i) should satisfy

$$R_{\min} \leq \sqrt{(x_i - x_h)^2 + (y_i - y_h)^2} \leq R_{\max} \tag{10}$$

2.3. Fitness Function Design. In the construction of fitness function, the constraints in path planning should be divided into "elastic constraints" and "hard constraints." Elastic constraints include the air defense threat and flight offset. Hard constraints refer to rigid constraints such as terrain constraints and target locations. For elastic constraints, the fitness of a single point has little effect on the full path. The evaluation of the path quality mainly depends on the superposition of each point's elastic fitness value, so the fitness value of a single point is small. For hard constraints, the single-point fitness value has a greater influence on the path evaluation. If a certain point does not satisfy one of the hard constraints, the whole path will be abolished.

2.3.1. Fitness Design of a Flight Path. The fitness of a path is formulated as follows:

$$W_q = p + s + z \tag{11}$$

where P is the path offset, s is the distance of the path, and z is the penalty value of a terrain barrier.

If $\sqrt{(x_i - x_{oi})^2 + (y_i - y_{oi})^2} \geq r_i$ then z=∞; the path is to be abolished if it passes through the terrain obstacle area.

2.3.2. Threat Fitness Design. The path threat fitness is

$$W_t = W_f - J, \tag{12}$$

where W_f is the penalty value of an air defense threat and J is the reward value from bombing. Positive W_t means that threat is higher than reward, the risk of bombing the target is too high, and the path should be abolished, and vice versa.

(1) Design of penalty value for air defense threats: we set the serious threat area of air defense r and the general threat area R. The range of threat W_t is P~50 when the aircraft is in any of the serious threat areas, Q~P when it is in the general threat area, and 0~Q when it is outside the radar effective detection range.

When $L < r$,

$$W_{ij} = 50 - (50 - P) \times \frac{L}{r}. \tag{13}$$

When $r < L < R$,

$$W_{ij} = P - (P - Q) \times \left(\frac{L - r}{R - r}\right). \tag{14}$$

When $R < L$,

$$W_{ij} = Q \times \left(1 - \left(\frac{L - R}{L}\right)\right). \tag{15}$$

The threat value is the summation of each path point threat

$$W_f = \sum_{\substack{i=1 \\ j=1}}^{n} W_{ij}. \tag{16}$$

(2) Target reward value design: in order to highlight the progressive relationship between the target points, a design method of target reward value combined with the analytic hierarchy process (AHP) is proposed.

When the path point (x_i, y_i) is located at the bombardment location satisfying $R_{\max} \geq \sqrt{(x_i - x_h)^2 + (y_i - y_h)^2} \geq R_{\min}$, the reward value of this point is

$$J_i = C_i \cdot W_{ft}, \tag{17}$$

where W_{ft} is the acceptable threat value of the mission, which is determined by the aircraft's survival and penetration ability, and $C = \{C_1, C_2, C_3 ... C_4\}$, $C_1 + C_2 ... + C_N = 1$ are the target values.

There are many ways to determine the target value. According to different sources of original data, they can be divided into two categories: subjective weighting method and objective weighting method. The difference between the two methods is whether the subjective factors of decision maker are considered. In military field, the evaluation of targets involves many factors, such as tactical intention, commander consideration, and mission impact. These make it difficult to quantify the targets mathematically. Therefore, it is more appropriate to use the subjective weighting method. The subjective weighting method includes Delphi Method, AHP, Binomial Coefficient, and Decision Alternative Ratio Evaluation System (DARE). AHP [10] is a multi-objective decision analysis method combining qualitative and quantitative analysis. In particular, it quantifies the decision-makers' judgment based on experience when the target (factor) structure is complex and lacks necessary data. Compared with other methods, the AHP has the advantages of conciseness, practicability, and high efficiency. At the same time, it also has some limitations, such as excessive influence of subjective factors, low precision, and the inability to generate new solutions. But in the problem of determining the target value, there are the following characteristics. (1) The subjective factors of the planners are very important. (2) The error of the target accuracy has little effect on the fitness value. (3) There is a high requirement for the speed. (4) The problem only needs to rank the original targets and does not need new solutions. In summary, the AHP method is used to determine the target value.

First, the planner compares the targets in pairs. The comparison results are then used to evaluate the relative importance between the pair targets through a score table. The importance is ranked from 1 to 7, where 1 means less important and 7 means extremely important. For N=4, the target comparison table is shown in Table 1.

We can see that Table 1 is an m=4 order square matrix. We calculate the weight according to an analytic hierarchy process.

Table 1: Target comparison table.

Bomb target	Goal 1	Goal 2	Goal 3	Goal 4
Goal 1	C_{11}	C_{12}	C_{13}	C_{14}
Goal 2	C_{21}	C_{22}	C_{23}	C_{24}
Goal 3	C_{31}	C_{32}	C_{33}	C_{34}
Goal 4	C_{41}	C_{42}	C_{43}	C_{44}

First we find the 1/m power $\overline{C_i}$ of the product of every row element in matrix,

$$\overline{C_i} = \prod_{j=1}^{m} \left(C_{ij}\right)^{1/m}. \tag{18}$$

The target weight $\overline{C_i}$ is

$$C_i = \frac{\overline{C_i}}{\sum_{i=1}^{m} \overline{C_i}}. \tag{19}$$

A single target reward value can be obtained from (17), (18), and (19),

$$J_i = \frac{\prod_{j=1}^{m} \left(C_{ij}\right)^{1/m}}{\sum_{i=1}^{m} \prod_{j=1}^{m} \left(C_{ij}\right)^{1/m}}. \tag{20}$$

The target reward value of the entire path is

$$J = \sum_{i=1}^{N} J_i. \tag{21}$$

2.4. Model Optimization. A multi-target strike path optimization model is established based on the above analysis:

$$\begin{gathered} \min\left(W_q\right); \\ \min\left(W_t\right); \\ \sqrt{\left(x_i - x_{oi}\right)^2 + \left(y_i - y_{oi}\right)^2} \geq r_{oi} + 1; \\ R_{\max} \leq \sqrt{\left(x_i - x_h\right)^2 + \left(y_i - y_h\right)^2} \leq R_{\min}; \\ W_f \leq W_{ft}; \end{gathered} \tag{22}$$

3. The Hybrid Conjugate Gradient Method for MOEA/D Algorithm

In the actual multi-target path planning, the target position and parameters, battlefield environment, etc. often change rapidly. A hybrid conjugate gradient method (MCGM) MOEA/D algorithm is proposed to solve the problem of reprogramming in finite time when the task parameters change.

3.1. MOEA/D Algorithm. MOEA/D algorithm simplifies the multi-objective problem into several single-objective problems by using a decomposition strategy [11]. Compared with the traditional evolutionary algorithm, the subproblems do not need to be optimized repeatedly, and the adjacent subproblems can be optimized with each other to improve the efficiency of the algorithm [12, 13]. However, because the algorithm needs a large population size, the convergence speed is low when the subproblem becomes complex.

3.2. The Conjugate Gradient Method. The conjugate gradient method [14] is a deterministic algorithm based on the steepest descent method [15] and the Newton method [16]. Compared with Newton's method, it does not need to compute Hesse matrix and has good quadratic termination, but it is easy to fall into a local minimum when solving optimization problems.

The algorithm flow is as follows.

Step 1. Set the algorithm precision ε, $k = 1$, and select the initial search point $x^{(1)}$.

Step 2. The algorithm termination condition is $\|\nabla f(x^{(k)})\| \leq \varepsilon$. If it is established, the algorithm will terminate; otherwise

$$d^{(k)} = -\nabla f\left(x^{(k)}\right) + \beta_{k-1} d^{(k-1)} \tag{23}$$

β_{k-1} :

$$\beta_{k-1} = \begin{cases} 0, & k = 1 \\ \dfrac{\left\|\nabla f\left(x^{(k)}\right)\right\|^2}{\left\|\nabla f\left(x^{(k-1)}\right)\right\|^2}, & k > 1 \end{cases} \tag{24}$$

Step 3. One-dimensional search is carried out to solve a_k by minimizing:

$$\min \varphi(a) = f\left(x^{(k)} + a d^{(k)}\right) \tag{25}$$

Set $x^{(k+1)} = x^{(k)} + a_k d^{(k)}$;

Step 4. Set $k = k + 1$; turn to step 2.

3.3. The Improved MOEA/D Algorithm

3.3.1. Analysis of Improved MOEA/D Algorithm. According to the characteristics of the two algorithms, an improved MOEA/D algorithm is proposed by combining the two algorithms.

At present, some studies have incorporated the conjugate gradient method into the evolutionary algorithm. For example, [17, 18] proposed the conjugate gradient method as a search operator to improve the search speed of the algorithm. In [17], the conjugate gradient method is used to search all individuals in the population, which results in excessive computation and a loss of speed advantage. In [18], in order to reduce the computational complexity, the population central individual (population mean individual) is used as the initial search point. Although this method improves the efficiency of the algorithm, in the case of large population, a single central individual cannot represent the entire population, and the solution is easy to fall into local optimal solutions.

To overcome the shortcomings of the above methods, this paper proposes an initial search point selection method with Gauss perturbations. The algorithm improves the speed while retaining the excellent convergence.

3.3.2. Selection of Initial Search Points for Adding Gauss Perturbation. In statistics, the larger the size of the data is, the closer the data distribution is to normal distribution. Under the condition of a large population, the population distribution can be regarded as normal distribution. Gauss perturbation refers to the stochastic perturbations that satisfy normal distribution. In this paper, a Gaussian perturbation is added to the selection of initial search points, and the number of search points is properly increased, so that the set of search points has the probability distribution characteristics of the population.

Given the population size m, the individual $a_i \in R, (i = 1, 2, ...m)$, the central individual a_0 is the average of individual fitness in the population,

$$a_0 = \frac{1}{m}\sum_{i=1}^{m} a_i. \tag{26}$$

Assuming that the population satisfies the normal distribution of (a_0, σ^2) and that a_0 is the average of individual population, $\mu = a_0$, σ^2 can be obtained from the variance formula

$$\sigma^2 = \frac{1}{m}\sum_{i=1}^{m} \left(a_i - a_0\right)^2. \tag{27}$$

The initial search point a_0^{i} is generated after adding Gaussian perturbations to the center population

$$a_0^{\mathrm{i}} = a_0 + gauss\left(a_0, \sigma^2\right) \tag{28}$$

Repeat 10 times to generate the initial search point set $\{a_0^{\mathrm{i}}\}(i = 1, 2...10)$. The set $\{a_0^{\mathrm{i}}\}$ thus has the probability distribution characteristics of the population, which not only ensures the diversity of sampling, but also avoids searching for all individuals, so that the algorithm will easily fall into local optimum while increasing the speed.

3.3.3. The Improved MOEA/D Algorithm Flow. The improved MOEA/D algorithm flow is as follows.

Step 1. Algorithm initialization.

Step 2. Neighbor selection among individuals.

Step 3. Mutual optimization among neighbors.

Step 4. Calculate the fitness of individuals and calculate the population center a_0.

Step 5. The initial search point set a_0^i is generated, and the conjugate gradient method is used to search. After satisfying the termination condition, the search result set a_n^i is obtained.

Table 2: Target value comparison.

bomb target	target 1	target 2	target 3	target 4
target 1	1	1	3	1/3
target 2	1	1	3	1/3
target 3	1/3	1/3	1	1/5
target 4	3	3	5	1

Table 3: Simulation parameter table.

Task parameters
Target coordinates: (35,20) (45,60)
(55,70) (80,90)
Target value: C_1=0.20 C_2=0.20
C_3=0.07 C_4=0.520
Acceptable threat value: 60
Radar coordinates: (20,30) (56,80)
Radar threat radius: R=15 R=20
Radar severe threat radius: r=7 r=6
Terrain threat coordinates:(60,20) (55,40) (70,40)
Terrain threat radius: R=15 R=15 R=20
Flight speed: 720km/h
Minimum turning radius of aircraft: 1.1km
Operational radius: 500km
Algorithm parameter setting
Population size: 150
Neighbor size: 30
Maximum number of iterations: 500
Number of decision variables: 34

Step 6. a_n^i is used to generate new individuals and calculate fitness values, and the individuals whose fitness values are lower than the new individuals will be replaced.

Step 7. Determine whether the loop ends or not by using the termination condition; if not, turn to step 2 to repeat the cycle until the end of the loop.

4. Simulation Results and Analysis

In order to verify the planning ability of the model under different situations, four simulation experiments are designed to four situations.

4.1. Setting of Simulation Parameters. The battlefield scope is set at 100 km × 100 km, and the target comparison evaluation table is shown in Table 2.

The target weight is $C_1 = 0.20$, $C_2 = 0.20$, $C_2 = 0.20$, $C_3 = 0.07$, $C_4 = 0.520$.

The Simulation parameters are shown in Table 3 .

4.2. Algorithm Performance Analysis. The improved MOEA/D algorithm and the traditional MOEA/D algorithm are used to solve the model and make the first path planning in MATLAB 2014. If the algorithm Pareto curve is smooth and no longer changing, the algorithm has converged. In order

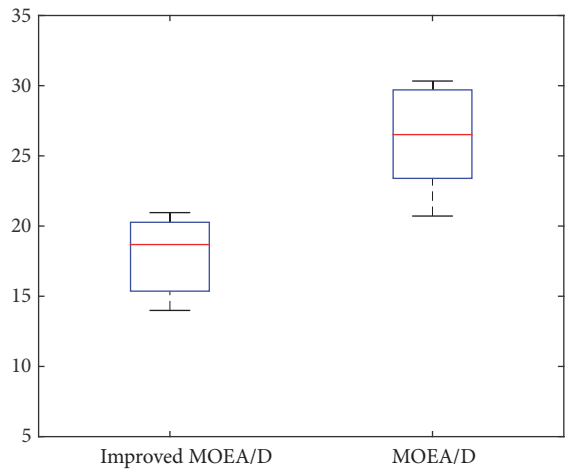

Figure 2: Convergence time box diagram.

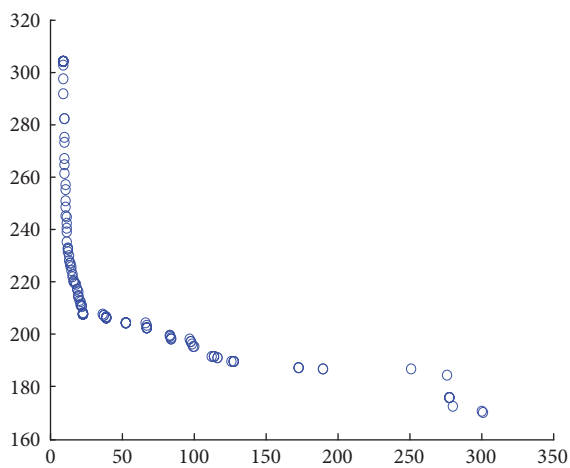

Figure 3: The x-axis represents the fitness of path and uses the "Wp" in the formula (11) to indicate. The y-axis represents the threat fitness and uses the "Wt" in the formula (12) to indicate.

to compare the convergence speeds of the two algorithms, 20 simulation experiments were carried out to record the convergence time of the two algorithms, and a box diagram of the convergence time was shown in Figure 2.

Figure 2 shows that the median convergence time of the improved MOEA/D algorithm is 18s, while that of the traditional MOEA/D algorithm is 26s. On the stability of the receiving speed, the upper and lower bounds of the improved MOEA/D algorithm are 14s-21s and the difference is 7s, while the upper and lower bounds of the MOEA/D algorithm are 21s-31s and the difference is 10s. In summary, the improved MOEA/D algorithm has better convergence speed and stability.

Taking the median convergence rate of the algorithm as the data, the Pareto front-end diagrams of the improved MOEA/D algorithm and the traditional MOEA/D algorithm are shown in Figures 3 and 4.

By analyzing Figures 3 and 4, we can see that the shape of Pareto curves of the two algorithms is basically similar, and

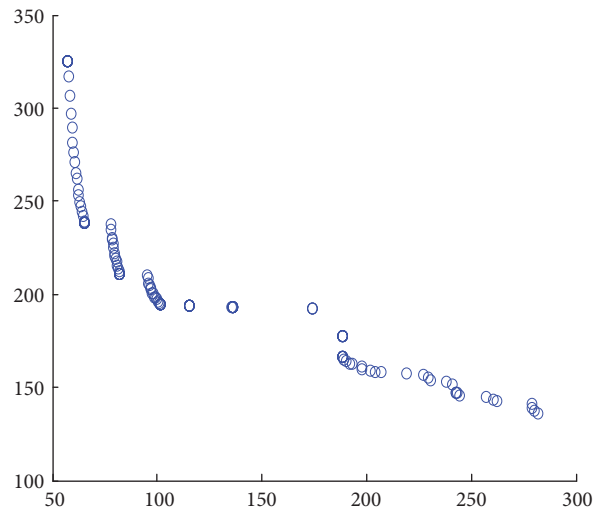

Figure 4: MOEA/D algorithm Pareto front-end diagram.

the improved MOEA/D algorithm has better continuity and smoothness.

4.3. Path Analysis. The four situations correspond to (1) striking high-threat and low-value targets, (2) target points in an insurmountable terrain barrier, (3) striking remote target points, and (4) striking high-threat high-value targets. The path planning modeling approach proposed in [6] is used as the first and second situation simulation experiment control group. It verifies the importance of the aircraft performance and the path threat to selected targets. The third and fourth experiments verify the path planning ability under different conditions of the model.

4.3.1. The First Situation Path Analysis. We use the Pareto front-end diagram to analyze the first path planning solved by the improved MOEA/D algorithm. If the range problem is a given priority, the optimal flight path distance of the aircraft is 144 km and the threat value is 148. If the priority is given to the aircraft safety, the flight path distance of the aircraft is 295 km and the threat value is 18. In order to balance the two factors, the median individuals of the population are selected to plot the path. The path planning map is shown in Figure 5.

The circle in the figure represents the radar threat. The outer circle is the general threat area. The inner circle is the serious threat area. If an aircraft enters the serious threat area, it will have a greater probability of being shot down. The interior part filled with oblique lines is the overlooking section of terrain obstacles at flight altitude. The fly path must not pass through this area. The points (C_1, C_2, C_3, C_4) in the figure indicate the target that the mission needs to bomb, and the path should reach the area where it can be bombed. Analysis of Figure 5 shows that the path effectively evades the threat, shortens the range as much as possible, and passes through the targets C_1, C_2, and C_4. Because of the low value of the target and the serious threat, the bombing cost of the aircraft is too high for C_3, so the model abandons the target

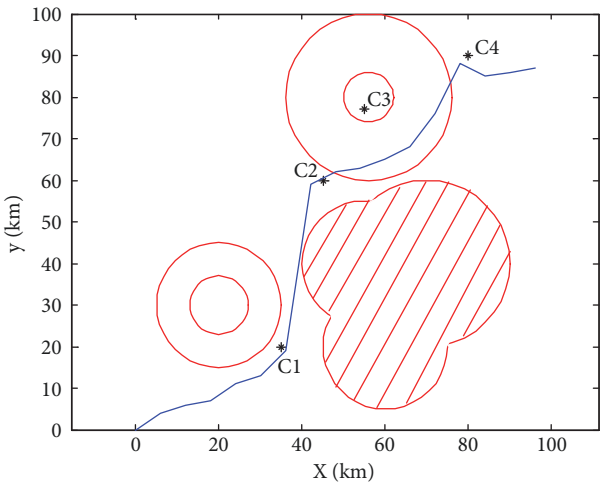

Figure 5: The path planning result in the first situation.

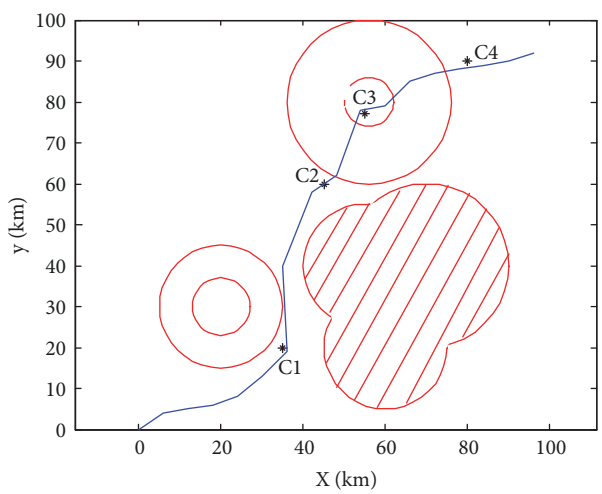

Figure 6: The path planning result of the control group in the first situation.

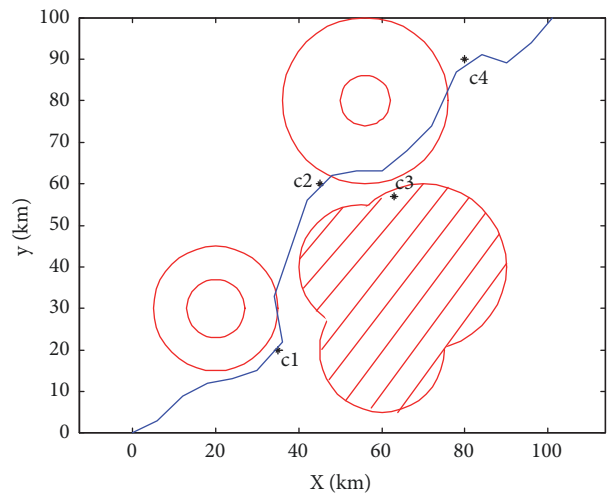

Figure 7: The path planning result for the second situation.

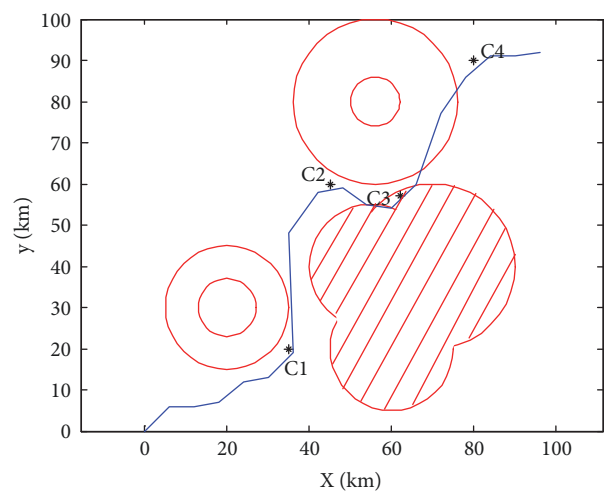

Figure 8: The path planning result of control group in the second situation.

C_3. The calculated flight path threat value is 36, which is less than 60 that the aircraft can tolerate.

Figure 6 shows the path planned by the model of the control group. The planned path also evades the threats and passes through the targets C_1, C_2, C_3, and C_4. The calculated flight path threat value is 104, which is far more than the aircraft's tolerance, 60. If the flight path is executed, the aircraft will be shot down with a high probability.

4.3.2. The Second Situation Path Analysis. Remove the target C_3 from the serious threat area and place C_3 in terrain obstacle which the aircraft is difficult to overcome. The coordinates are (62, 57) and the paths planned by the two approaches are shown in Figures 7 and 8, respectively.

In Figure 7, although striking C_3 does require an aircraft to go through the serious threat area, the aircraft cannot exceed the terrain obstacles, so striking C_3 is given up.

As shown in Figure 8, the path entered the terrain obstacle directly. This is inadvisable.

4.3.3. The Third Situation Path Analysis. Move the target point C_3 in the serious threat area to a coordinate point (100, 70) that is not threatened but is relatively far from the central axis of the path. The path has been replanned, shown in Figure 9.

Figure 9 shows that although the target C_3 is relatively remote, the path can still pass through the area that leads to the elimination of C_3.

4.3.4. The Fourth Situation Path Analysis. If C_3 is a high value target, we can adjust the acceptable threat value and the value of target point C_3. Here we set the targets C_3=0.55 C_1=0.15 C_2=0.15 C_4 =0.15, and the affordable threat value W_{ft} = 150. The simulated flight path planning is shown in Figure 10.

In Figure 10, comparing the results of the first and the second path planning, the model plans a different path under the condition that the basic battlefield environment remains unchanged, but the target value and the aircraft's tolerance of

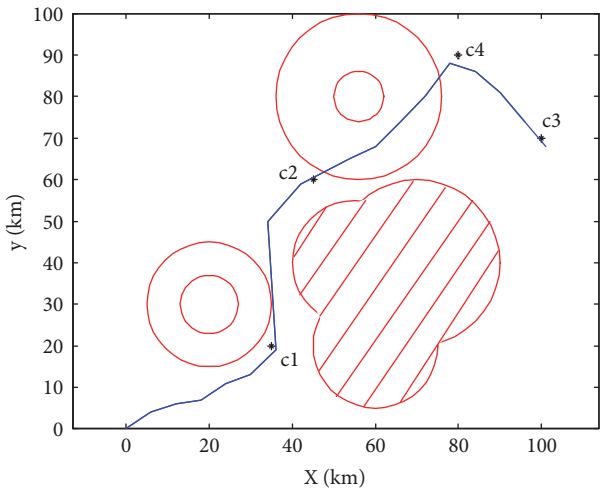

Figure 9: The path planning result in the third situation.

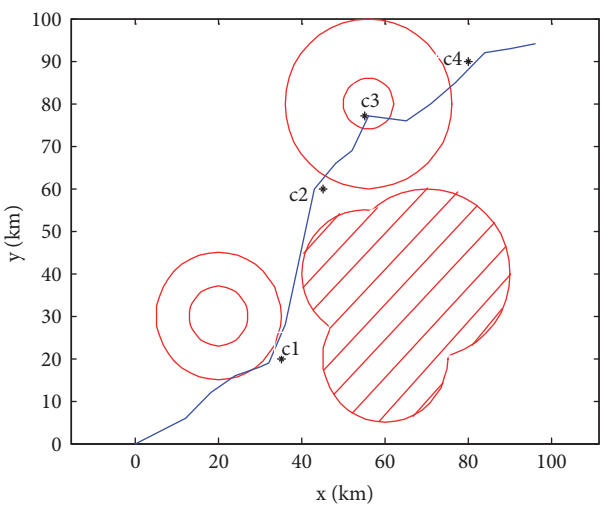

Figure 10: The path planning result in the fourth situation.

threat have changed. When the aircraft is faced with a high-threat and low-value target C_3, it abandons the target. When the aircraft has an improved ability to withstand threats and C_3 becomes a high-value target, the model plans a path which includes C_3.

By analyzing the first and second simulation experiments, the importance of selecting targets based on the value of target, aircraft performance, and threats was proved by the comparison with the control group. Compared with the path of the control group that strikes all targets, the modeling approach proposed in this paper has more practicability. The third and fourth experiments show that the path planned by the model in this paper can strike any target on the premise of ensuring the safety of the aircraft.

5. Conclusion

This paper discusses and solves the flying path planning problem for multi-target missions. The proposed method evaluates the weight of each target using the analytic hierarchy process (AHP) and determines the value for each target after considering the aircraft's acceptable threat tolerance. The improved MOEA/D algorithm is used to solve the problem of target selection and path planning. The simulation results show that the improved algorithm can converge quickly and better. By adjusting the weight of the target value and the acceptable threat tolerance, we can obtain a path that satisfies the mission requirements. We use a simple multi-target bombing mission as an example, but the method can be easily extended to other situations with different constraints on the target region and fly parameters.

Data Availability

The data used to support the findings of this study are available from the corresponding author upon request.

Conflicts of Interest

The authors declare that there are no conflicts of interest regarding the publication of this paper.

Authors' Contributions

Ming Zhong planned the work, completed the simulation experiment, and drafted the main part of the paper. RenNong Yang contributed to error analysis. Huan Zhang and Jun Wu contributed to setup type.

Acknowledgments

The work described in this paper is partially supported by the National Natural Science Foundation of China under Grant No. 61503405.

References

[1] X.-L. Ma, W. Ye, and H.-D. Fan, "Research of computer simulation on route planning of low altitude penetration," *Xitong Fangzhen Xuebao / Journal of System Simulation*, vol. 16, no. 3, p. 458, 2004.

[2] Z.-H. Peng, J.-P. Wu, and J. Chen, "Three-dimensional multi-constraint route planning of unmanned aerial vehicle low-altitude penetration based on coevolutionary multi-agent genetic algorithm," *Journal of Central South University of Technology (English Edition)*, vol. 18, no. 5, pp. 1502–1508, 2011.

[3] L. Liu and S. Zhang, "Voronoi diagram and GIS-based 3D path planning," in *Proceedings of the 2009 17th International Conference on Geoinformatics*, pp. 1100–1104, Fairfax, Va, USA, August 2009.

[4] X. Zhang, J. Chen, and B. Xin, "Path planning for unmanned aerial vehicles in surveillance tasks under wind fields," *Journal of Central South University*, vol. 21, no. 8, pp. 3079–3091, 2014.

[5] W. Cai, M. Zhang, and Y. R. Zheng, "Task assignment and path planning for multiple autonomous underwater vehicles using 3D dubins curves," *Sensors*, vol. 17, no. 7, 2017.

[6] L. C. Shen, Y. F Zhu, H. Y. Zhu et al., *Theories and Methods of Autonomous Cooperative Control for Multiple UAVs*, National Defense Industry Press, Beijing, China, 2013.

[7] R. Kala, A. Shukla, and R. Tiwari, "Dynamic environment robot path planning using hierarchical evolutionary algorithms," *Cybernetics and Systems*, vol. 41, no. 6, pp. 435–454, 2010.

[8] S. MahmoudZadeh, A. M. Yazdani, K. Sammut, and D. M. W. Powers, "Online path planning for AUV rendezvous in dynamic cluttered undersea environment using evolutionary algorithms," *Applied Soft Computing*, vol. 70, pp. 929–945, 2018.

[9] Q. Zhang and H. Li, "MOEA/D: a multiobjective evolutionary algorithm based on decomposition," *IEEE Transactions on Evolutionary Computation*, vol. 11, no. 6, pp. 712–731, 2007.

[10] J. Chen, *Mathematical Modeling and Mathematical Experiment*, Higher Education Press, Beijing, China, 2007.

[11] Y. Zhang, R. Yang, J. Zuo, and X. Jing, "Enhancing MOEA/D with uniform population initialization, weight vector design and adjustment using uniform design," *Journal of Systems Engineering and Electronics*, vol. 26, no. 5, pp. 1010–1022, 2015.

[12] D. W. Ding, *Research on the Application of Decomposition Based Multi-objective Evolutionary Algorithm (MOEA/D) in Antenna Optimization Design*, Jiangsu University, Zhenjiang, China, 2012.

[13] Q. Zhang, W. Liu, and H. Li, "The performance of a new version of MOEA/D on CEC09 unconstrained MOP test instances," in *Proceeding of the IEEE Congress on Evolutionary Computation (CEC '09)*, pp. 203–208, Trondheim, Norway, May 2009.

[14] J. S. Jiang, C. X. He, and S. H. Pan, *Optimization Computation Method*, South China University of Technology Press, Guangzhou, China, 2007.

[15] M. Gen and R. W. Cheng, *Genetic Algorithm and Engineering Design*, John Wiley & Sons, New York, NY, USA', 1997.

[16] D. Kim and J. A. Fessler, "Adaptive restart of the optimized gradient method for convex optimization," *Journal of Optimization Theory and Applications*, vol. 178, no. 1, pp. 240–263, 2018.

[17] X. Liang, W. Xiao, W. Long, and H. Qin, "Instructed-crossover genetic algorithm based on gradient information," *Journal of Computer Applications*, vol. 30, no. 10, pp. 2582–2584, 2010.

[18] J. Li, Y. Wang, G. Y. Li et al., "Fast Convergence of Hybrid Genetic Algorithm," *Computer Engineering and Design*, vol. 35, no. 2, pp. 686–689, 699, 2014.


Advances in Operations Research
Advances in Decision Sciences
Journal of Applied Mathematics
The Scientific World Journal
Journal of Probability and Statistics
International Journal of Mathematics and Mathematical Sciences
Hindawi
Submit your manuscripts at
www.hindawi.com
Journal of Optimization
International Journal of Engineering Mathematics
International Journal of Analysis
Journal of Complex Analysis
Advances in Numerical Analysis
Mathematical Problems in Engineering
International Journal of Differential Equations
Discrete Dynamics in Nature and Society
International Journal of Stochastic Analysis
Journal of Mathematics
Journal of Function Spaces
Abstract and Applied Analysis
Advances in Mathematical Physics